Stable Beamforming with Low Overhead for C/U-plane Decoupled HSR Wireless Networks

Li Yan, *Student Member, IEEE,* Xuming Fang, *Senior Member, IEEE,* and Yuguang Fang, *Fellow, IEEE*

***Abstract*—Millimeter wave (mmWave) directional communications have become a vital 5G technique to achieve the goal of multiple gigabit data rate with low latency , which also hold true for high speed railway (HSR) wireless networks. However, the high mobility in HSR scenarios causes frequent beam realignments and consequently high feedback overheads, degrading the transmission reliability and efficiency. In mmWave beamforming systems, besides transmitters (TXs), receivers (RXs) are also equipped with antenna arrays, which equivalently introduces a new degree of freedom for link adaptation. Based on this observation, a stable beamforming scheme with low overhead, consisting of both long-term TX beamforming and short-term RX beamforming, is proposed. In the long-term TX beamforming, under the premise of satisfying the basic receiver sensitivity (RS), TXs are devised to use as wide beams as possible to extend the serving time of each beam. In the short-term RX beamforming, within a TX beam, RXs autonomously adjust RX beams according to the current channel state information (CSI) instead of frequently feeding it back to TXs, thereby reducing feedback overheads and accelerating link adaptation. Through this scheme, the received signal to noise ratio (SNR) is kept at a high and stable level. To meet the strict transmission reliability requirements in HSRs, the control/user-plane (C/U-plane) decoupled architecture is applied to mitigate the inherent blindness of mmWave directional beams. Theoretical and numerical results show that the proposed scheme can significantly reduce feedback overheads and guarantee the desired performance.**

***Index Terms*—5G; C/U-plane decoupling; beamforming; millimeter wave; stability, HSR wireless networks**

I. Introduction

In future HSR systems, e.g., smart trains or artificial intelligence (AI) based high-speed trains, more and more devices with advanced control and communications, such as real-time video surveillance cameras, will be embedded in trains, which will generate tremendous data to be transmitted to group control centers. Onboard passengers also have a strong desire to get high-quality mobile services during long journeys. Therefore, how to increase the system capacity to fulfill these requirements becomes a significant factor to improve HSR. Nevertheless, the highly saturated lower frequency bands cannot shoulder this huge burden. Millimeter wave (mmWave) bands, spanning from 30 to 300GHz with massive ultra wideband spectra, have been viewed as the main enabler in achieving the goal of multiple gigabit data rate with low latency in future 5G systems [1]. In high speed railway (HSR) wireless communication networks, mmWave communications are also envisioned as a potential candidate to solve the demand issue on the ever increasing capability requirements resulting from the rapid development in the HSR industry [2], [3]. Nevertheless, higher frequency bands mean higher path loss, which is a dominating barrier of putting mmWave communications into practice. To deal with this challenge, the directional beamforming based on massive antennas becomes an enabling technology when coming to mmWave communications [4]. However, depending only on mmWave communications, which have the inherent blindness problem due to directional narrow beams, cannot satisfy the strict transmission reliability requirements in HSR scenarios [2]. Fortunately, in our previous works, we had demonstrated how a control/user-plane (C/U-plane) decoupled HSR wireless network can utilize reliable lower frequency bands to remedy the limited coverage problem in higher frequency bands [5]. In this paper, we use this architecture to facilitate operations over mmWave bands, such as control information exchanges. Even when the mmWave link quality degrades heavily, mobile relays (MRs) can still maintain their connections while reestablishing mmWave links via the control information exchanges on reliable and omnidirectional lower frequency bands. Note that to facilitate the understanding of this paper, we use long-term evolution (LTE) networks as a baseline for analysis.

Before the application of beamforming in mmWave communications, many researchers have already launched the study on using antenna arrays to wireless networks [6]. In the conventional space division multiple access (SDMA) systems that operate at microwave bands, base stations (BSs) are equipped with antenna arrays to form space-orthogonal beams to serve users simultaneously. With limited size, user terminals are usually equipped with a single antenna. In conventional SDMA systems, to adapt to various wireless channels, users have to frequently feed back their estimated downlink channel state information (CSI) to BSs and wait for the transmitter (TX) beam adjustments from BSs to improve the received signal quality. The beamforming scheme based on the conventional SDMA technique has also been developed in HSR wireless networks [7], [8]. In [7], a position information based route-tracking beamforming scheme was proposed for railway com-

L. Yan and X. Fang are with Key Lab of Information Coding & Transmission, Southwest Jiaotong University, Chengdu 610031, China. (E-mails: Liyan12047001@my.swjtu.edu.cn, xmfang@swjtu.edu.cn).

Y. Fang is with the Department of Electrical and Computer Engineering, University of Florida, PO Box 116130, Gainesville, FL 32611, USA. (E-mail: fang@ece.ufl.edu).

The work of L. Yan and X. Fang was supported partially by NSFC under Grants 61471303, and NSFC Guangdong Joint Foundation under Grant U1501255, and EP7-PEOPLE-2013-IRSES Project under Grant 612652. The work of Y. Fang was partially supported by the US National Science Foundation under Grant CNS-1717736.

munication systems. The field tests carried out over the Taiwan railway verified the performance improvements of this scheme. In [8], a two-stage beamforming gain scheme is proposed to improve the handover performance in railway scenarios. For clarity, in the subsequent analyses, we use the term "Previous scheme" to represent the scheme that adopted the conventional SDMA technique in railways. However, the frequent feedback based link adaptation method will not be suitable for fast-varying channels under high mobility scenarios.

Different from the conventional SDMA systems where only TX sides have enough space to accommodate large antenna arrays to form beams, the short wavelength of mmWave bands makes it also possible to equip users with antenna arrays under the same space volume. As a consequence, a user equipment (UE, e.g., CPE, rooftop transceivers) in mmWave communications is inherited with an ability to autonomously adjust receiver (RX) beams to adapt to various wireless channels, which equivalently introduces a new degree of freedom for link adaptation. Especially in HSRs, with a large space on trains, MRs can be equipped with massive antenna arrays and powerful computing processors to realize autonomous link adaptations, thereby mitigating the aforementioned problem. Besides, in most public mobile networks, the movement of users is random and the best way of beamforming is to use narrow beams to track them. Nevertheless, in HSR scenarios, the trajectory of a train is predetermined. To reduce beam adjustments, we can use wide beams to pre-cover the area that a train will go through. Based on the above analyses, we propose a stable beamformring scheme with low overhead which consists of two parts, namely, the long-term TX beamforming and short-term RX beamforming. In the long-term TX beamforming, while satisfying the basic RX sensibility, roadside mmWave remote radio units (mmW-RRUs) use as wide beam as possibile to extend each beam's serving time, so as to reduce the number of TX beam adjustments and therefore feedback overheads. In the short-term RX beamforming, MRs, deployed on the outside roof of trains to forward data between roadside RRUs and inside access points (APs), autonomously adjust RX beams according to the current estimated CSI instead of frequently feeding it back to mmW-RRUs, which greatly reduces feedback overheads and accelerates link adaptation. It should be noted that although two separate terms, i.e., long-term TX beamforming and short-term RX beamforming, are used in this paper to make the description more explicit, they are two closely related components of the entire scheme, in which the long-term TX beamforming guarantees the basic coverage while the short-term RX beamforming fine-tunes the received SNR to a desired stable level.

In HSR scenarios, especially in China, viaducts account for the vast majority of track deployments, leading to a much cleaner LOS propagation environment [9], Besides, by adopting beamforming, compared with the line of sight (LOS) link, non-line of sight (NLOS) components have negligible energy [10]. Usually, roadside mmW-RRUs have a certain distance to the railway tracks. When radiating to MRs deployed on outside roofs of trains, directional beams will also form a wide coverage area whose dimension is much larger than the overhead lines, which therefore can survive from the blockages of overhead lines. On the other hand, roadside overhead line pillars are usually about 6m high and lower than mmW-RRUs with a usual height of at least 10m, which thereby will not block the beams radiated from higher mmW-RRUs. Based on this observation, the effects of the power supply overhead line system on beam transmissions are not taken into account in this paper. Therefore, we assume the wireless channel in our scenario has only LOS links. After that, TX and RX beam directions can be determined based on the train position information which can be precisely predicted in HSR scenarios [7]. In addition, the regular movements and the predetermined trajectory of trains are also two specific characteristics in HSR scenarios, which will make it easier to execute beam tracking [2], [11], [12], [13]. Considering the undependable transmissions during beam adjustments and the inherent blindness of directional mmWave communications, the system is developed from the C/U-plane decoupled architecture which integrates relatively reliable lower frequency bands to guarantee the transmission reliability of important control information. Consequently, we can design the system in such a way that low frequency remote radio units (LF-RRU), operating at omnidirectional lower frequency bands, help MRs to forward the position information to mmW-RRUs. On the other hand, directional narrow beams tend to be very sensitive to positioning errors. Therefore, during beamwidth adjustments, we also take into account the effects of positioning errors on beam alignments, which may be caused by noises in positioning systems, errors or delay during wireless transmissions. Besides, when coming to the wireless communication systems in high mobility scenarios, the Doppler's effect is an inevitable issue. Nevertheless, in addition to the LOS characteristics of wireless channels in HSR which causes limited Doppler spread, based on the results from [14], using beamforming to confine the reception angle range at receivers can also reduce the Doppler spread. After that, according to [11], the dominating Doppler shift can be easily or even totally tracked and compensated due to the predictable regular movements of trains in HSRs.

Capacity stability is a key performance indicator (KPI) in wireless communications, which was overlooked in the previous works [15]. According to [16], the instable capacity in physical wireless links has caused a great deal of inefficiency in throughput and some other issues, such as the performance degradation in the over-wireless transmission control protocol (TCP). Therefore, it is necessary to consider the capacity stability as an important factor in future network designs, so as to mitigate the information starvation or congestions in higher layers. However, in HSR scenarios, trains run through the cellular coverage with such a high speed that the received signal quality experiences fast ups and downs, leading to serious capacity instability. To address this problem, in the proposed short-term RX beamforming, as trains move away from mmW-RRUs, MRs narrow down RX beams to increase the beamforming gain to compensate the resulting increasing path loss. Through the proposed scheme, the final received signal to noise ratios (SNRs) across the whole coverage of an mmW-RRU is kept at a high and stable level. On the other hand, with a stable SNR, TXs do not need to frequently change

modulation and coding schemes (MCSs) for users, thereby saving significant resource to inform users about the current used MCSs on downlink control channels.

To sum up, the main contributions of this paper are listed as follows.

1) We apply the C/U-plane decoupled architecture in future mmWave based HSR wireless networks by using reliable and omnidirectional lower frequency bands to mitigate the inherent blindness problem in mmWave directional communications.
2) We propose a stable beamforming scheme with low overhead which consists the long-term TX beamforming in mmW-RRUs and the short-term RX beamforming in MRs. While satisfying the basic receiver sensitivity (RS), mmW-RRUs use as wide beams as possible to extend the serving time of each beam, so as to reduce the number of TX beam adjustments. Within a TX beam, MRs autonomously adjust RX beams according to the current CSI instead of frequently feeding it back and waiting for the TX adjustments, reducing feedback overheads and accelerating link adaptation.
3) We formulate the objective of the proposed scheme as minimizing the gap between the final actual received SNR and a pre-defined target SNR. Through the proposed scheme, the final received SNR is kept at a high and stable level, improving the system capacity stability.
4) We conduct theoretical analyses and simulations to verify the effectiveness of our scheme. The results show that our proposed scheme can significantly reduce feedback overheads while achieving a stable transmission performance.

The remainder of this paper is organized as follows. In Section II, the detailed network architecture is depicted. In Section III, the optimization problems of the long-term TX beamforming and short-term RX beamforming are formulated and solved. In Section IV, numerical results are presented. Finally, Section V concludes this paper.

II. Network Architecture

To mitigate the inherent blindness problem in mmWave directional communications, the C/U-plane decoupled architecture is applied in this paper as we have done before [5]. To improve the network deployment flexibility and baseband resource utilization, cloud radio access networks (C-RANs) were introduced in future 5G networks. Based on this observation, network nodes in our system are deployed based on the C-RAN architecture. The detailed network architecture is shown in Fig. 1. Two types of RRUs are linearly deployed along the rail, in which LF-RRUs use omnidirectional antennas to establish the reliable and omnidirectional coverage, while mmW-RRUs adopt directional beamforming to overcome the path loss in mmWave bands. All RRUs are connected to a baseband unit (BBU) pool through high-speed backhauls. As for a train, an AP and an MR are deployed on the roofs inside and outside trains, respectively, so as to provide a dependable connection for train passengers. The inside AP firstly collects the services of train passengers, which then are forwarded to roadside BSs via MRs. In this way, the problems resulting from direct connections between onboard passengers and roadside base stations, such as the large penetration loss and group handovers, can be addressed. To increase capacity while maintaining reliability, the relatively important C-plane between MRs and wireless networks is reserved at LF-RRUs operating over reliable lower frequency bands, while the counterpart U-plane is moved to mmW-RRUs operating over ultra broadband mmWave bands.

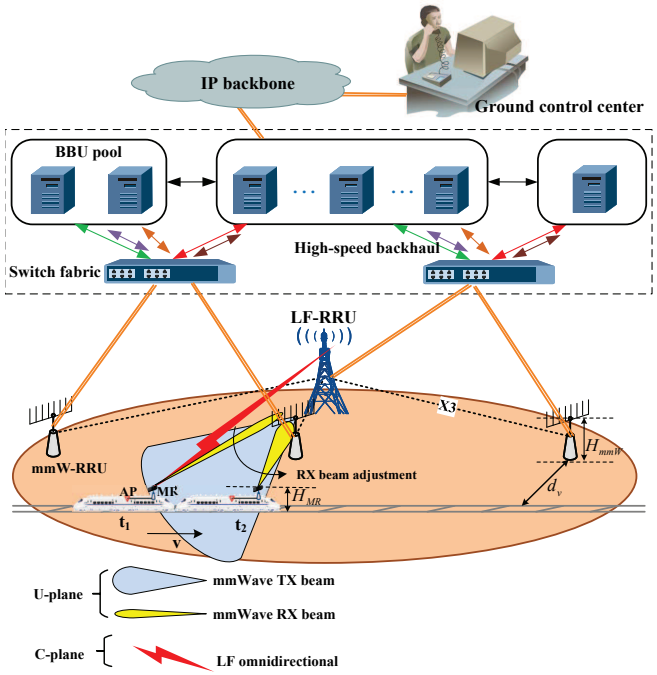

Fig. 1. Network architecture.

At the beginning of studying beamforming techniques in railway wireless networks, roadside BSs are equipped with antenna arrays to form TX beams, while MRs are equipped with a single receive antenna [6], [7], [8]. For clarity, we call it "Previous scheme" in the following contents. In the previous scheme, with LTE as the baseline, MRs need to periodically feed back the position information and CSIs to BSs and wait for TX beam adjustments from BSs to improve the received signal quality. Nevertheless, in high mobility scenarios, frequent feedback-based link adaptation always confronts with the problem of feedback information expiration due to the feedback delay. In mmWave communications, besides TXs, RXs are also equipped with antenna arrays. In other words, RXs also have the ability to adapt to various wireless channels by adjusting the RX beams. Based on this observation, we propose to use the long-term TX beamforming in mmW-RRUs and the short-term RX beamforming in MRs. Different from the previous scheme, in the proposed scheme the TX and RX beamwidth are not fixed. Under the premise that the basic receive sensitivity is satisfied, mmW-RRUs use TX beams with as wide beamwidth as possible to extend the serving time of each beam. Within a TX beam, MRs autonomously adjust RX beams according to current CSIs instead of frequently feeding them back, to reduce feedback overheads and accelerate link adaptation. Fig. 2 shows the link

adaptation differences between two schemes.

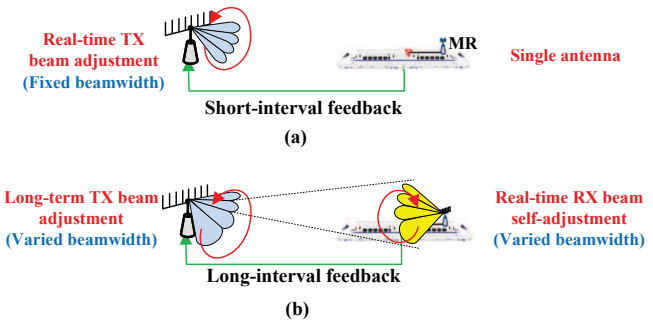

Fig. 2. Link adaptation. (a)In the previous scheme, MRs need to frequently feed back CSIs to mmW-RRUs and wait for TX beam adjustments from mmW-RRUs to obtain satisfied received signal quality. (b) In the proposed scheme, within a TX beam, MRs autonomously adjust RX beams according to CSIs instead of frequently feeding them back.

For simplicity, the downlink is taken as a case study in this paper. Nevertheless, the concept of exploiting the link adaptation freedom in receiver sides that are equipped with antenna arrays can also be generalized to the uplink. At first, MRs storage the positions of all roadside mmW-RRUs in advance. Then, combining this information and the current position information of its own, an MR can orientate the direction of the next TX beam. The receiver sides of the uplink are mmW-RRUs which usually have more powerful processors to do more complicated tasks of estimating both the direction and gain of wireless channels [17]. Based on the estimation results, mmW-RRUs can autonomously adjust the direction and beamwidth of RX beams to keep the final SNR at a high and stable level.

III. Mathematical Models

In this section, the optimization problems of the long-term TX beamforming in mmW-RRUs and the short-term RX beamforming in MRs are formulated and solved. Through the proposed scheme, the total feedback overheads are reduced and the final received SNRs are kept at a high and stable level across the whole coverage of an mmW-RRU.

A. The Long-term TX Beamforming

Based on [18], a trackable expression of the beamforming gain can be given by

$$G\left(\theta_b, \Delta\theta\right) = \frac{2\pi}{\theta_b} e^{-\eta\left(\frac{\Delta\theta}{\theta_b}\right)^2}, \tag{1}$$

where θ_b is the 3dB beamwidth. $\Delta\theta{=}\alpha{-}\mu$ is the angle difference between the main lobe direction α and the user's azimuth μ. η is a constant value and equal to $4\log 2$.

In most public mobile networks, since the movements of users are unpredictable, it is more efficient to point the main lobe of TX beams towards users. The situation is quite different in HSR wireless networks. The trajectories and movement directions of trains are predefined and known in advance. Hence, it is reasonable to point the main lobe towards the front areas of MRs when conducting TX beam adjustments as shown in Fig. 3, so as to extend the serving time of each TX beam. In Fig. 3(a), the previous scheme uses TX beamforming with fixed beamwidth and a single antenna for receiving. Obviously, in the regions near mmW-RRUs, since the path loss is not high, it causes significant energy waste to use high-gain narrow beams. In the proposed long-term TX beamforming scheme as shown in Fig. 3(b), while satisfying the basic receive sensitivity, mmW-RRUs form TX beams with as wide beamwidth as possible to avoid energy waste and extend the serving time of each beam. In Fig. 3, d_{min} is the smallest signal propagation distance between trains and mmW-RRUs, which can be expressed as $d_{\min} = \sqrt{d_v^2 + \left(H_{mmW} - H_{MR}\right)^2}$, where as shown in Fig. 1 d_v is the vertical distance between the track and mmW-RRUs, and H_{mmW} and H_{MR} are the heights of mmW-RRUs and trains, respectively. BSP_i and L_i are the beam switching points and the coverage distance, respectively, with definitions detailed next.

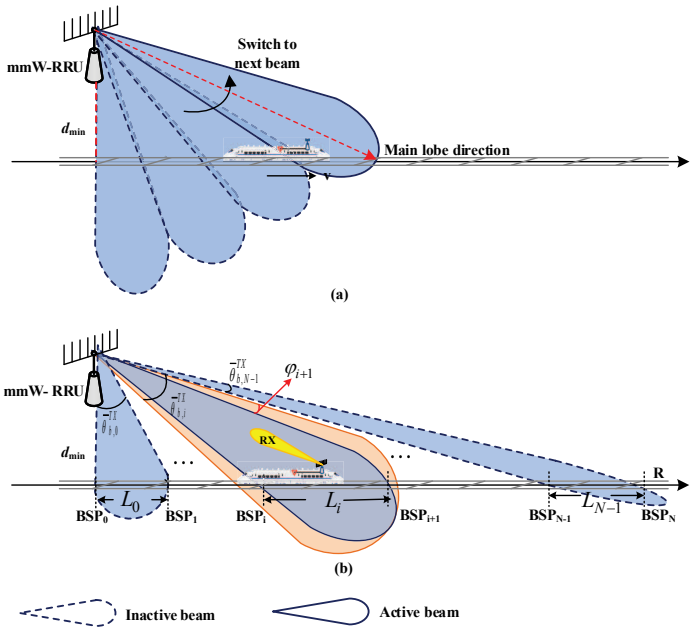

Fig. 3. Illustration of beamforming schemes. (a) The previous scheme with TX beamforming of the fixed beamwidth and a single antenna for receiving, (b) The proposed scheme with adaptive TX and RX beamwidth.

Definition 1 (Beam switching point, BSP): The intersection between a TX beam's boundary and the track is defined as a beam switching point, at which when an MR arrives the mmW-RRU will switch its TX beam to the next one. The original beam switching point, denoted as BSP_0, is the projection of the mmW-RRU on the track as depicted in Fig. 3(b). Then, along with the MR's movement trajectory which is defined as the x-axis, the coordinate values of beam switching points can be expressed as

$$BSP_i = \begin{cases} 0, i = 0 \\ \sum_{j=0}^{i-1} L_j, i = 1, 2, 3, ..., N \end{cases} \tag{2}$$

where N denotes the total number of TX beams, and L_j is the effective beam coverage defined as follows.

Definition 2 (Effective beam coverage): The effective beam coverage is defined as the projection region of a TX beam on the track in which receivers can correctly receive and decode the data. Outside the effective beam coverage, the signal strength of a beam will be too low to provide correct reception.

Proposition 1: Consider a linear movement trajectory of MRs with starting at BSP_0, the effective beam coverage of the TX beam i can be given by

$$L_i = \begin{cases} \tan\left(\theta_{b,0}^{TX}\right) \cdot d_{\min}, i = 0 \\ \left(\tan\left(\sum_{j=0}^{i} \theta_{b,j}^{TX}\right) - \tan\left(\sum_{j=0}^{i-1} \theta_{b,j}^{TX}\right)\right) \cdot d_{\min}, \\ i = 1, 2, 3, ..., N \end{cases} \tag{3}$$

where $\theta_{b,i}^{TX}$ represents the beamwidth of the TX beam i.

Proof: See Appendix A. ■

In HSR scenarios, especially in China, viaducts account for the vast majority of track deployments, leading to a much cleaner LOS propagation environment [9]. Moreover, by adopting directional beamforming, NLOS components will have very low energy that can be directly neglected [10]. Based on this observation, we can use the MR's position information to guide MRs and mmW-RRUs in pairing their beams, which will greatly reduce beam training overheads and accelerate link establishments. However, in practical systems, positioning errors, which may be caused by noises in positioning systems, errors or delay during transmissions, cannot be ignored when using position information for beam alignments. In the worst case, positioning errors may even lead to connection drops. To solve this problem, as shown in Fig. 3(b), an extra guard angle (GA), denoted as φ_i, is considered at both boundaries of TX beams in the proposed long-term TX beamforming scheme.

Next, we will first present the relationship between positioning errors in distance and the counterpart angle errors. After that, the communication outage probability of the proposed scheme with guard angles at boundaries of TX beams is derived. For clarity, Fig. 4 shows the geometric relationship between positioning errors in distance and the counterpart angle errors, where $\Delta\mu_i$ is the angle error and $D_i = \sqrt{d^2_{\min} + BSP_i^2}$ is the distance between the mmW-RRU and BSP_i.

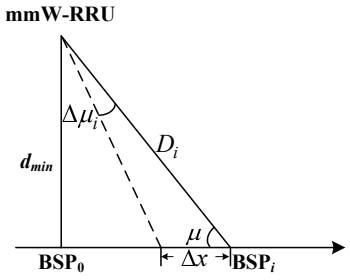

Fig. 4. Positioning error analysis.

Proposition 2: At BSP_i, the relationship between the positioning error Δx in distance and its counterpart angle error $\Delta\mu_i$ can be approximately depicted as

$$\Delta x \approx \frac{\Delta\mu_i \cdot D_i^2}{d_{\min}}. \tag{4}$$

Proof: See Appendix B. ■

Assuming that the positioning error in distance follows the Gaussian distribution with zero mean and $\sigma^2_{\Delta x}$ variance, according to the result in (4), we can get $\Delta\mu_i \sim N\left(0, \frac{d^2_{\min}}{D_i^4}\sigma^2_{\Delta x}\right)$.

Definition 3 (Outage due to TX beam misalignment): Due to positioning errors, TX beams of mmW-RRUs may miss the target MR, leading to connection drops, which is defined as outage due to TX beam misalignment.

Proposition 3: Consider an extra angle φ_i reserved at both boundaries of the TX beam i. The outage due to TX beam misalignment will take place with probability

$$P_{out,i}(\varphi_i) = \Pr(\Delta\mu_i > \varphi_i) = Q\left(\frac{D_i^4 \cdot \varphi_i}{d^2_{\min} \cdot \sigma^2_{\Delta x}}\right). \tag{5}$$

Proof: From (4), $\Delta\mu_i$ follows the Gaussian distribution, i.e., $\Delta\mu_i \sim N\left(0, \frac{d^2_{\min}}{D_i^4}\sigma^2_{\Delta x}\right)$, then $\Pr(\Delta\mu_i > \varphi_i) = \int_{\varphi_i}^{+\infty} \frac{D_i^4}{2\pi d^2_{\min}\sigma^2_{\Delta x}} e^{-\Delta^2\mu_i/2\left(\frac{d^2_{\min}}{D_i^4}\sigma^2_{\Delta x}\right)^2} d\Delta\mu_i$. For clarity, we simplify the expression in (5) by using the well-known Q function defined as $Q(x) = \frac{1}{2\pi}\int_x^{+\infty} e^{-\frac{y^2}{2}} dy$. ■

To control the communication outage probability under the predefined threshold Γ_{out}, we can get the required guard angle as

$$\varphi_i = \frac{d^2_{\min}\sigma^2_{\Delta x} h}{D_i^4}, \tag{6}$$

where $h = Q^{-1}(\Gamma_{out})$ is a constant value that can be found in [19] if Γ_{out} is determined.

For simplicity, we reserve the same angles on both sides of TX beams, that is

$$\varphi_{i+1} = \varphi_i = \max\left(\frac{d^2_{\min}\sigma^2_{\Delta x} h}{D_i^4}, \frac{d^2_{\min}\sigma^2_{\Delta x} h}{D_{i+1}^4}\right) = \frac{d^2_{\min}\sigma^2_{\Delta x} h}{D_i^4} \tag{7}$$

Taking guard angles into account, the actual TX beamwidth becomes

$$\overline{\theta}_{b,i}^{TX} = \theta_{b,i}^{TX} + 2\varphi_i \tag{8}$$

In the long-term TX beamforming, while satisfying the basic receive sensitivity, mmW-RRUs form TX beams with as wide beamwidth as possible to extend the serving time of each beam, thereby reducing feedback overheads caused by frequent TX beam adjustments. If the feedback overhead is β bits every time, the optimization problem to minimize the total feedback overheads of the long-term TX beamforming within the coverage of an mmW-RRU can be formulated as

$$\begin{aligned} &\min_{\theta_{b,i}^{TX}} \beta \cdot N, i = 0, 1, 2, ..., N \\ &s.t. \\ &C1: \textstyle\sum_{i=0}^{N-1} \theta_{b,i}^{TX} \geq a\tan\left(\frac{R}{d_{\min}}\right) \\ &C2: \theta_{b,\min}^{TX} \leq \overline{\theta}_{b,i}^{TX} \leq \theta_{b,\max}^{TX} \\ &C3: Pt - PL\left(\textstyle\sum_{j=0}^{i} L_j\right) + 10\lg\left(G\left(\overline{\theta}_{b,i}^{TX}, \frac{\theta_{b,i}^{TX}}{2}\right)\right) \geq \gamma, \end{aligned} \tag{9}$$

where N is the total number of beam switchings, which also represents the number of feedbacks. Since the feedback overhead every time is constant, the objective function is equivalent to minimizing N. There are three constraints in this optimization problem. C1 guarantees the total effective coverage of all TX beams to be not smaller than a required value, i.e., the coverage radius R. C2 keeps the TX beamwidth within the scope determined by the maximum and minimum available beamwidths. C3 ensures that the received SNRs of MRs anywhere within the TX beam i are not lower than the basic receiver sensitivity. In the expression of C3, Pt and γ are the mmW-RRU transmit power and the receiver sensitivity, respectively. $PL(x)$ represents the path loss when the MR locates at x which can be given by [20]

$$PL(x) = 32.4 + 20\log_{10} f_c + 20\log_{10}\sqrt{d_{\min}^2 + x^2}, \quad (10)$$

where f_c is the frequency in gigahertz. The measurement of d_{min} and x is in meters.

Within the TX beam i, when the MR is at the right boundary, i.e., BSP_{i+1}, the signal propagation distance is the largest and the beamforming gain is the lowest, which means the MR suffers from the worst case at BSP_{i+1}. If at BSP_{i+1} the received signal quality is guaranteed to be not smaller than the basic receiver sensitivity, the received SNRs in all other positions within the TX beam i can also be guaranteed.

Proposition 4: Based on results in (1), (3), and (10), we can derive the relationship between the left part of C3 and the beamwidth of the TX beam i as shown in (11) at the bottom of this page.

Proof: From (1), as the TX beamwidth $\theta_{b,i}^{TX}$ decreases, the beamforming gain $G\left(\overline{\theta}_{b,i}^{TX}, \frac{\theta_{b,i}^{TX}}{2}\right)$ increases. From (3), as $\theta_{b,i}^{TX}$ decreases, the effective coverage L_i also decreases. From (10), as L_i decreases, the path loss $PL\left(\sum_{j=0}^{i} L_j\right)$ also decreases. In summary, we can conclude that the left part of C3, i.e., $Pt - PL\left(\sum_{j=0}^{i} L_j\right) + 10\lg\left(G\left(\overline{\theta}_{b,i}^{TX}, \frac{\theta_{b,i}^{TX}}{2}\right)\right)$, increases as $\theta_{b,i}^{TX}$ decreasing. In other words, the left part of C3 is a monotonic decreasing function of $\theta_{b,i}^{TX}$. ■

To minimize the total number of beam switchings N, under the constraints C2 and C3, the beamwidth $\theta_{b,i}^{TX}$ should be as wide as possible. Consequently, the solution to the long-term TX beamforming optimization problem is described in Algorithm 1, where δ_{TX} is the step size.

After getting $\theta_b^{TX}(i)$, the BSPs within the coverage of mmW-RRUs can be determined based on (2). Then, LF-RRUs can forward these results to MRs in advance. When getting close to these BSPs, MRs will feed back the position information to LF-RRUs. After LF-RRUs forward the position information to mmW-RRUs, mmW-RRUs will adjust TX beams to the pre-devised beamwidth and directions. Fig. 5 depicts the detailed signaling procedures. Based on the above analysis, we find that, given the transmit power and the coverage radius of mmW-RRUs, the smallest signal propagation distance between trains and mmW-RRUs, the maximum and the minimum reachable beamwidth, the TX beam switching points and the corresponding TX beamwidth of the proposed long-term TX beamforming scheme can be predetermined offline. Therefore, the computational complexity of the long-term TX beamforming algorithm is not considered in this paper.

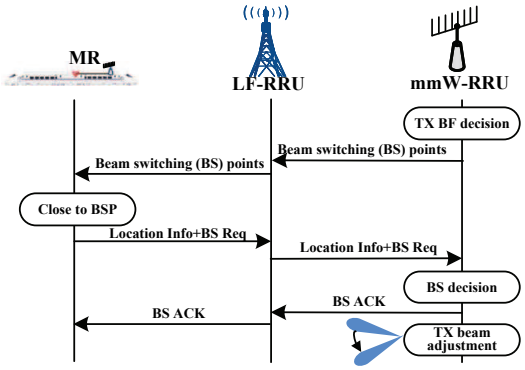

Fig. 5. The long-term TX beamforming signaling procedures.

B. The Short-term RX Beamforming

As aforementioned, in order to guarantee the system efficiency and throughput, the capacity stability should be viewed as a KPI in future wireless network designs [15]. However, in HSR scenarios, due to the high mobility the received signal quality degrades rapidly as trains leave BSs, which heavily affects the capacity stability. To solve this problem, the short-term RX beamforming scheme can be applied in MRs to smooth out the fast variations. Within the basic coverage provided by the long-term TX beamforming, MRs autonomously adjust RX beams to adapt to various wireless channels to keep final received SNRs at a predefined high and stable level.

Definition 4 (RX beam adjustment period): Denote the coherence time of wireless channels in HSR scenarios as T_c, over which the signal propagation characteristics can be viewed as coherent. To adapt to diverse wireless channels in real time, MRs need to adjust RX beams with a period of the same value of T_c, named the RX beam adjustment period.

Definition 5 (Outage due to RX beam misalignment): Similar to Definition 3, due to positioning errors, RX beams of MRs may also miss signals radiated from mmW-RRUs, thereby

$$\left.\begin{array}{l} G\left(\overline{\theta}_{b,i}^{TX}, \frac{\theta_{b,i}^{TX}}{2}\right) \propto \frac{1}{\theta_{b,i}^{TX}} \\ L_i \propto \theta_{b,i}^{TX} \\ PL\left(\sum_{j=0}^{i} L_j\right) \propto L_i \end{array}\right\} \Rightarrow \left(Pt - PL\left(\sum_{j=0}^{i} L_j\right) + 10\lg\left(G\left(\overline{\theta}_{b,i}^{TX}, \frac{\theta_{b,i}^{TX}}{2}\right)\right)\right) \propto \frac{1}{\theta_{b,i}^{TX}}. \quad (11)$$

leading to connection drops, which is defined as the outage due to RX beam misalignment. In the proposed short-term RX beamforming, MRs adjust RX beam directions and beamwidth in real time according to their self-supporting position information and estimated downlink CSIs, respectively. Different from the long-term TX beamforming, RX beam adjustments occur more frequently. To gain a higher RX beamforming gain, MRs should point the main lobe of RX beams towards mmW-RRUs. Under this condition, once the angle error, which is the counterpart of positioning errors in distance, is greater than the half of the RX beamwidth, communication outage will happen.

Proposition 5: With the main lobe of RX beams pointing to mmW-RRUs, the probability that the angle error is greater than the half beamwidth of RX beams is the communication outage probability given below

$$P_{out}\left(\theta_b^{RX,i}\right)=\Pr\left(\Delta\mu>\frac{\theta_b^{RX,i}}{2}\right)=Q\left(\frac{R_i^4\cdot\theta_b^{RX,i}}{2\sigma_{\Delta x}^2\cdot d_{\min}^2}\right), \tag{12}$$

where $R_i=\sqrt{d_{\min}^2+i\cdot T_c\cdot v}$ denotes the distance between an MR and an mmW-RRU when the MR executes the ith RX beam adjustment.

Proof: The proof is similar to that of Proposition 3. ■

Definition 6 (Average channel gain): In beamforming systems, at a given time, the beam attributes including beamwidth and directions are determined by the current CSI and location information, respectively. However, mmWave bands have a broad spectrum with diverse channel gains on different subcarriers. Therefore, in this paper, we use the average channel gain, which is the average value of all subcarriers' channel gains, as the basis to guide the RX beam adjustments.

Take LTE networks as a baseline where users can obtain downlink CSIs by estimating reference signal sequences inserted in downlink frames [21]. Suppose that L reference signals are inserted in the whole spectrum, each of which provides a CSI, denoted as β_k, to describe the signal propagation characteristics of subcarriers around this reference signal. The average channel gain of the whole spectrum can be calculated as $\overline{\beta}=\frac{1}{L}\sum_{k=0}^{L-1}\beta_k$. Note here that the wireless channel gain β_k results from the joint effect of the path loss, small-scale fading and TX beam gain, which can be expressed as

$$\beta_k=PL\left(x\right)+10\log_{10}G\left(\overline{\theta}_b^{TX},\frac{\theta_b^{TX}}{2}\right)+10\log_{10}s_k, \tag{13}$$

where s_k is the gain of small-scale channels which follows Rician distribution in LOS scenarios [22].

Definition 7 (Average RX beamforming gain): Although in the short-term RX beamforming MRs can adjust RX beams more frequently, an RX beam still has to be sustained for at least an RX beam adjustment period. During this time, the MR may have moved a long distance, leading to a significant angle shift on the original aligned beam pair. Based on this observation, to simplify the theoretical analysis, we define the average RX beamforming gain as the average value of RX beamforming gains on this angle shift.

Proposition 6: According to (4), the angle shift corresponding to the movement distance of an MR during the ith RX beam adjustment period can be obtained as $\varpi_i=\frac{T_c\cdot v\cdot d_{\min}}{{R_i}^2}$. By averaging the RX beamforming gains on this angle shift, that is,

$$\begin{aligned}\overline{G\left(\theta_b^{RX,i}\right)}&=\tfrac{1}{\varpi_i}\int_0^{\varpi_i}G\left(\theta_b^{RX,i},\Delta\theta\right)d\Delta\theta\\&=\tfrac{c}{\varpi_i}\left(\Phi\left(\tfrac{\varpi_i}{\theta_b^{RX,i}/\sqrt{2\eta}}\right)-\tfrac{1}{2}\right),\end{aligned} \tag{14}$$

where $c=2\pi\sqrt{\frac{\pi}{\eta}}$ and $\Phi\left(x\right)=\frac{1}{\sqrt{2\pi}}\int_{-\infty}^{x}e^{-t^2/2}dt$, we can use this result to simplify the following theoretical analysis.

Proof: See Appendix C. ■

To keep the final received SNR around a predefined value SNR_{tar}, the short-term RX beamforming optimization problem can be formulated as

$$\begin{aligned}&\min_{\theta_b^{RX,i}}\left|\frac{Pt\cdot\overline{G\left(\theta_b^{RX,i}\right)}\cdot\overline{\beta_i}}{N_0}-SNR_{tar}\right|\ i=0,1,2....,\left\lceil\frac{R}{T_c\cdot v}\right\rceil\\&s.t.,\begin{cases}\mathrm{C1}:\theta_{\min}^{\mathrm{RX}}\le\theta_b^{RX,i}\le\theta_{\max}^{\mathrm{RX}}\\\mathrm{C2}:\theta_b^{RX,i}\ge\frac{2T_c\cdot v\cdot d_{\min}}{{R_i}^2}\\\mathrm{C3}:P_{out}\left(\theta_b^{RX,i}\right)\le\Gamma_{out}\end{cases}.\end{aligned} \tag{15}$$

To guarantee the capacity stability, the objective in (14) is to minimize the gap between the actual SNRs and the target SNR. There are three constraints in this problem. C1 restricts the RX beamwidth between the allowable maximum and minimum values. Since the main lobe of RX beams is pointed to mmW-RRUs, C2 is required to make sure that the half beamwidth of RX beam i can support the possible movement distance of MRs in one adjustment period. Due to C3, the selected RX beamwidth controls the communication outage probability under the threshold Γ_{out}. Based on the above analyses, the three constraints can be combined into one as

$$\max\left(\theta_{\min}^{\mathrm{RX}},\frac{2T_cvd_{\min}}{{R_i}^2},\frac{2h\sigma_{\Delta x}^2d_{\min}^2}{R_i^4}\right)\le\theta_b^{RX,i}\le\theta_{\max}^{\mathrm{RX}}. \tag{16}$$

Algorithm 1: The long-term TX beamforming

Input $Pt,d_{\min},R,\theta_{b,\max}^{TX},\theta_{b,\min}^{TX},\delta_{TX},h$;
initialize $\theta_{sum}=0,i=0,N=0,D\left(0\right)=d_{\min}$;
while $\theta_{sum}<a\tan\left(\frac{R}{d_{\min}}\right)$ **do**
  $\varphi\left(i\right)=\frac{d_{\min}^2\sigma_{\Delta x}^2h}{D(i)^4}$;
  $\overline{\theta}_b^{TX}\left(i\right)=\theta_{b,\max}^{TX}$;
  $\theta_b^{TX}\left(i\right)=\theta_{b,\max}^{TX}-2\varphi\left(i\right)$;
  while $Pt-PL\left(\tan\left(\sum_{j=0}^{i}\theta_b\left(j\right)\right)\cdot d_{\min}\right)+10\lg\left(G\left(\overline{\theta}_b^{TX}\left(i\right),\frac{\theta_b^{TX}(i)}{2}\right)\right)<\gamma$ **do**
    $\theta_b^{TX}\left(i\right)=\theta_b^{TX}\left(i\right)-\delta_{TX}$;
    $\overline{\theta}_b^{TX}\left(i\right)=\max\left(\overline{\theta}_b^{TX}\left(i\right)-\delta_{TX},\theta_{b,\min}^{TX}\right)$;
  end while
  $\theta_{sum}=\theta_{sum}+\theta_b^{TX}\left(i\right)$;
  $i=i+1$;
  $N=N+1$;
  $D\left(i\right)=d_{\min}\sqrt{1+\tan\theta_{sum}^2}$;
end while
Output $\theta_b^{TX}\left(i\right),N$;

Obviously, when $\frac{Pt\cdot\overline{G\left(\theta_b^{RX,i}\right)}\cdot\overline{\beta_i}}{N_0}=SNR_{tar}$, the objective function reaches the minimum value of zero. By substituting (13), we can get the corresponding RX beamwidth as $\theta_{b,temp}^{RX,i}=\frac{\varpi_i\cdot\sqrt{2\eta}}{\Phi^{-1}\left(\frac{\varpi_i\cdot SNR_{tar}\cdot N_0}{Pt\cdot\overline{\beta_i}\cdot c}+\frac{1}{2}\right)}$. However, we must ensure that the obtained value does satisfy the comprehensive constraint in (15). If it is true, then $\theta_b^{RX,i}=\theta_{b,temp}^{RX,i}$. Otherwise, since the actual SNR is a linear function of beamforming gain and $\overline{G\left(\theta_b^{RX,i}\right)}\propto\frac{1}{\theta_b^{RX,i}}$, if $\theta_{b,temp}^{RX,i}>\theta_{\max}^{\mathrm{RX}}$, $\theta_b^{RX,i}=\theta_{\max}^{\mathrm{RX}}$. Similarly, if $\theta_{b,temp}^{RX,i}<\max\left(\theta_{\min}^{\mathrm{RX}},\frac{2T_c\cdot v\cdot d_{\min}}{{R_i}^2},\frac{2h\cdot\sigma_{\Delta x}^2\cdot d_{\min}^2}{R_i^4}\right)$, then $\theta_b^{RX,i}=\max\left(\theta_{\min}^{\mathrm{RX}},\frac{2T_c\cdot v\cdot d_{\min}}{{R_i}^2},\frac{2h\cdot\sigma_{\Delta x}^2\cdot d_{\min}^2}{R_i^4}\right)$. The solution to the short-term RX beamforming optimization problem is given in Algorithm 2. It is easy to observe that with the self-estimated CSI in mmW-RRUs, the RX beamwidth can be directly determined by solving a simple equation. Although the result needs to satisfy the constraint in (16), the process only involves three simple calculations witholut introducing any iterations. Consequently, the online short-term RX beamforming algorithm has a very low computation complexity, which thereby can be applied to high mobility scenarios. Besides, we observe that only when the channel gain satisfies $\frac{N_0\cdot SNR_{tar}}{Pt\cdot G(\theta_{\max}^{RX})}\le\overline{\beta_i}\le\frac{N_0\cdot SNR_{tar}}{Pt\cdot G\left(\theta_{\min,i}^{final}\right)}$ can the MR reach the target SNR through RX beam adjustments. Otherwise, the MR still needs to feed back the current CSI to the mmW-RRU, based on which mmW-RRU adjusts the target SNR. The detailed operations are not discussed in this paper, but left to our future work.

The related signaling procedures of the short-term RX beamforming scheme are given in Fig. 6. Based on the demanded target SNR from mmW-RRUs, MRs do the RX beam adjustments. As aforementioned, only when the channel gain satisfies $\frac{N_0\cdot SNR_{tar}}{Pt\cdot G(\theta_{\max}^{RX})}\le\overline{\beta_i}\le\frac{N_0\cdot SNR_{tar}}{Pt\cdot G\left(\theta_{\min,i}^{final}\right)}$ can the MR reach the target SNR through RX beam adjustments. Otherwise, as shown in Fig. 6, the MR still needs to feed back the current CSI to the mmW-RRU, based on which the mmW-RRU adjusts the target SNR. If the reachable highest SNR of the narrowest RX beamwidth is still lower than the predefined target SNR, mmW-RRUs will lower the target SNR to maintain the capacity stability. On the other hand, if MRs can further narrow down RX beams to gain a higher SNR, a higher target SNR will be sent to MRs. Besides, in conventional wireless systems, base stations have to readjust MCSs in time to adapt to the wireless channel changes, and use additional resources in downlink control channels to inform users of the current used MCS [23], while, in the proposed scheme, the final SNRs are always kept at a stable level. In the proposed scheme, transmitters do not need to frequently change MCSs while receivers adapt the receive beamwidth to compensate for the path loss, and thus, many resources for notifications are saved.

Algorithm 2: The short-term RX beamforming

Input $Pt,\overline{\beta_i},R_i,\varpi_i,SNR_{tar},T_c,v,\sigma_{\Delta x}^2,\Gamma_{out},\theta_{\min}^{RX},\theta_{\max}^{RX},h$;

1: **calculate** $\frac{2T_cvd_{\min}}{{R_i}^2}$, $\frac{2h\sigma_{\Delta x}^2d_{\min}^2}{R_i^4}$ and $\frac{\varpi_i\sqrt{2\eta}}{\Phi^{-1}\left(\frac{\varpi_iSNR_{tar}N_0}{Pt\overline{\beta_i}c}+\frac{1}{2}\right)}$;

2: **let** $\theta_{\min,i}^{final}=\max\left(\theta_{\min}^{\mathrm{RX}},\frac{2T_cvd_{\min}}{{R_i}^2},\frac{2h\sigma_{\Delta x}^2d_{\min}^2}{R_i^4}\right)$ and $\theta_{b,temp}^{RX,i}=\frac{\varpi_i\cdot\sqrt{2\eta}}{\Phi^{-1}\left(\frac{\varpi_i\cdot SNR_{tar}\cdot N_0}{Pt\cdot\overline{\beta_i}\cdot c}+\frac{1}{2}\right)}$;

3: **if** $\theta_{\min,i}^{final}\le\theta_{b,temp}^{RX,i}\le\theta_{\max}^{\mathrm{RX}}$ **then**

4: $\theta_b^{RX,i}=\theta_{b,temp}^{RX,i}$;

5: **elseif** $\theta_{b,temp}^{RX,i}>\theta_{\max}^{\mathrm{RX}}$ **then**

6: $\theta_b^{RX,i}=\theta_{\max}^{\mathrm{RX}}$;

7: **else**

8: $\theta_b^{RX,i}=\theta_{\min,i}^{final}$;

9: **end if**

10: **Output** $\theta_b^{RX,i}$;

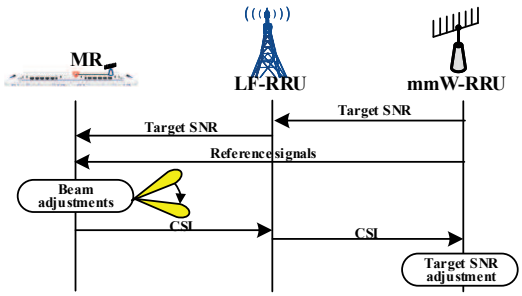

Fig. 6. The short-term RX beamforming signaling procedures.

IV. Numerical Results

In this section, numerical analysis is used to demonstrate the effectiveness of the proposed scheme in reducing feedback overheads while maintaining capacity stability. The baseline comparison is with the previous scheme in which mmW-RRUs use fixed and narrow beams and MRs use single antenna for reception. In the proposed scheme, mmW-RRUs use wide beams to provide the basic coverage and MRs use adaptive RX beamforming to guarantee the desired received SNRs. Consequently, in both cases, only one of the transmitter and receiver sides provides a high beamforming gain, which to some degrees guarantees the comparison fairness. The parameter settings are listed in Table I [22], [24].

In Fig. 7, the TX beamwidth results of the two schemes are illustrated, where the curve titled "Long-term TX beamforming-BW with GAs" describes the TX beamwidth results with GAs, while the curve titled "Long-term TX beamforming-Effective BW" shows the effective TX beamwidth without GAs. The basic receiver sensitivity in this study is set to RS=-68dBm. As shown in Fig. 7, in the previous scheme, mmW-RRUs use fixed beamwidth with an appropriate value to provide dependable signal quality even when MRs are in the edge region. Nevertheless, the selected beamwidth is too narrow for the regions near mmW-RRUs, resulting in frequent TX beam adjustments. In the proposed scheme, mmW-RRUs can adaptively adjust the TX beamwidth to compensate diverse path losses in different regions. In the regions near mmW-RRUs, the beamforming gain of a wide beam is enough to compensate the relative low path loss, thereby extending the TX beam's serving time. While in the

TABLE I
PARAMETER SETTING

Parameters	Values
MmW-RRU transmit power	30dBm
MmW-RRU coverage radius	500m [24]
MmW-RRU frequency band	32GHz
d_v	20m
H_{mmW}	10m [24]
H_{MR}	3m [24]
Target SNR	40dB
SNR threshold	8dB
Rician factor of small-scale fading	10dB [22]
Maximum beamwidth ($\theta^{RX}_{\max} = \theta^{TX}_{\max}$)	30^o
Minimum beamwidth ($\theta^{RX}_{\min} = \theta^{TX}_{\min}$)	2^o
Noise figure	10dB
Noise power	-174dBm/Hz [24]
Positioning error variance	3m
Outage threshold	10^{-6}
Bandwidth	1GHz
Coherence bandwidth	20MHz
MR velocity	360km/h
Coherence time	10ms

edge regions, mmW-RRUs use narrow beams to overcome the path loss. Overall, the total number of feedbacks are reduced. Besides, from Fig. 7, we observe that as the MR moves away from the mmW-RRU, the angle error caused by the same positioning error in distance decreases accordingly. Therefore, the corresponding guard angle also decreases, which can be reflected from the gradually narrowing gap between the curves "Long-term TX beamforming-BW with GAs" and "Long-term TX beamforming-Effective BW". Note that Fig. 7 only presents the TX beamwidth results of different schemes, based on which the number of feedbacks can be reflected. In terms of the comprehensive reception quality, it will be analyzed later.

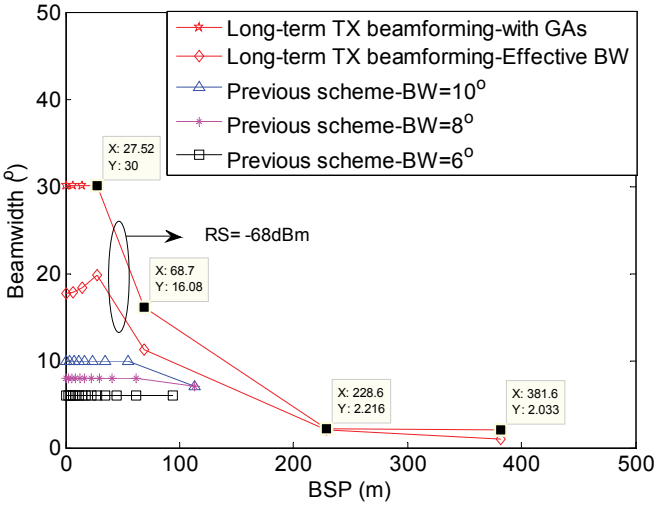

Fig. 7. TX beamwidth.

Table II lists the number of TX beam adjustments. For fairness, it is assumed that in the previous scheme only when MRs move to BSPs could a feedback message carrying the position information is sent to mmW-RRUs to request TX beam switch. Based on the simulation results in Fig. 7, we can clearly see that the proposed long-term TX beamforming scheme can reduce the number of TX beam adjustments, thereby also reducing the number of feedback messages.

The TX beamwidth and the number of feedbacks under three different receiver sensitivity conditions, i.e., RS=-82dBm, RS=-74dBm and RS=-68dBm, are illustrated in Fig. 8. In the region near mmW-RRUs, the selected TX beamwidth in three cases are the same, since the path loss is not very severe, using the maximum TX beamwidth can provide enough beamforming gain to attain a required signal quality. However, in edge regions, the three cases present different performance. With the receiver sensitivity getting stricter, the TX beamwidth decreases, thereby increasing the number of feedbacks.

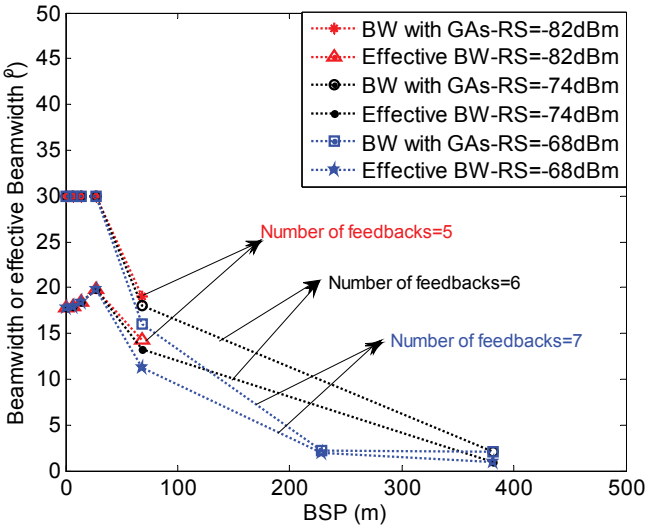

Fig. 8. Performance of the proposed long-term TX beamforming scheme under different receiver sensitivity conditions.

Next, we will conduct study for the combined performance of both the long-term TX beamforming and the short-term RX beamforming. Fig. 9(a) and 9(b) respectively show the final attained SNRs and the capacity stability of different schemes. From Fig. 9(a), we observe that in the previous scheme, a maximum SNR appears right after a TX beam adjustment. Nevertheless, as MRs move away from mmW-RRUs, the received SNR decreases. When the received SNR cannot satisfy the minimum SNR requirement, mmW-RRUs will switch the TX beam to the next one. From the overall point of view, despite the frequent ups and downs, the entire SNR degrades when MRs move away from mmW-RRUs. In the proposed scheme, since the path loss is very low in the regions near mmW-RRUs, constrained by the maximum available TX beamwidth, mmW-RRUs cannot use a wider TX beam than the maximum one, leading to a higher SNR

TABLE II
FEEDBACK COMPARISONS

Name	Number of TX adjustments
Proposed scheme	7
Previous scheme-10^o	9
Previous scheme-8^o	11
Previous scheme-6^o	14

than the predefined value. As MRs move to the edge regions, the final SNR is kept around the predefined value, thereby guaranteeing the capacity stability. Note that in this paper we do not consider the target SNR adjustments, but using a constant pre-defined target SNR in simulations. Hence, in the regions near mmW-RRUs of Fig. 9(a), the actual obtained SNR is higher than the target one.

For fairness, in Fig. 9(a) the curve titled "Fixed RX BW-5.7^o" gives the SNR performance of the scheme with fixed RX beamwidth. To maintain seamless connections, the selected beamwidth should not be narrower than the one that can support the moving distance of MRs in an RX beam adjustment period, i.e., $\theta_{fixed}^{RX} \geq \max_{R_i}\left(\frac{2T_c \cdot v \cdot d_{\min}}{{R_i}^2}\right) = \frac{l2T_c \cdot v}{d_{\min}}$. Substituting the parameter values into the above expression, we get $\theta_{fixed}^{RX} \geq 5.7^o$ and we use the RX beamwidth of 5.7^o to maximize the final received SNR. From the numerical results, we find that when MRs are near mmW-RRUs, the received SNR of the scheme with fixed RX beamwidth is higher than that of the proposed scheme. Nevertheless, when MRs move away from mmW-RRUs, the received SNR decreases and becomes lower than that of the proposed scheme. Starting from the point A marked in Fig. 9(a) where the mmW-RRU adjusts its TX beam, the received SNR of the scheme with fixed RX beamwidth outperforms that of the proposed scheme again. Until the point B where the mmW-RRU switch its TX beam to the next one, the received SNR of the scheme with fixed RX beamwidth is reduced to lower values. From the above results, we can see that the scheme with fixed RX beamwidth presents more obvious fluctuations in received SNR that cannot satisfy the capacity stability requirement.

For clarity, we define the stability factor as the expression $\mathrm{S}\,(d) = \frac{|SNR(d) - E(SNR(d))|}{E(SNR(d))}$, where d is the moving distance of MRs. Based on the definition, we can easily find that the closer to 0 the value of $S(d)$ is, the more stable the received SNR is. In Fig. 9(b), we can see from the results that the proposed scheme can provide the most stable service compared with others.

In Fig. 10(a) , the RX beamwidth of the proposed scheme is depicted. In Fig. 10(b), the communication outage probabilities of the two schemes with adaptive RX beamwidth and with fixed RX beamwidth, respectively, are illustrated. In the following, we will give a comprehensive analysis based on the two figures. When MRs are in the region near mmW-RRUs, a wide RX beam can provide the required RX beamforming gain to reach the target SNR. Besides, we can see from Fig. 10(b) that a wide beam can reduce the communication outage probability caused by positioning errors. Based on the geometric relationship in Fig. 4, we observe that in the region near mmW-RRUs, the same positioning error in distance can cause a higher angle error than that in the edge regions. Hence, although the scheme with fixed RX beamwidth experiences a higher communication outage probability when MRs are near mmW-RRUs, the situation gets better when MRs move to the edge. As MRs leave mmW-RRUs, the RX beamwidth of the proposed scheme also gets narrower. The three obvious turning points marked in Fig. 9(a) correspond to the three positions where mmW-RRUs adjust TX beams which are also marked in Fig. 7. Since a TX beam adjustment can improve the received signal quality, to keep the actual SNR around the target SNR, the RX beamwidth gets wider instead, leading to a turning point.

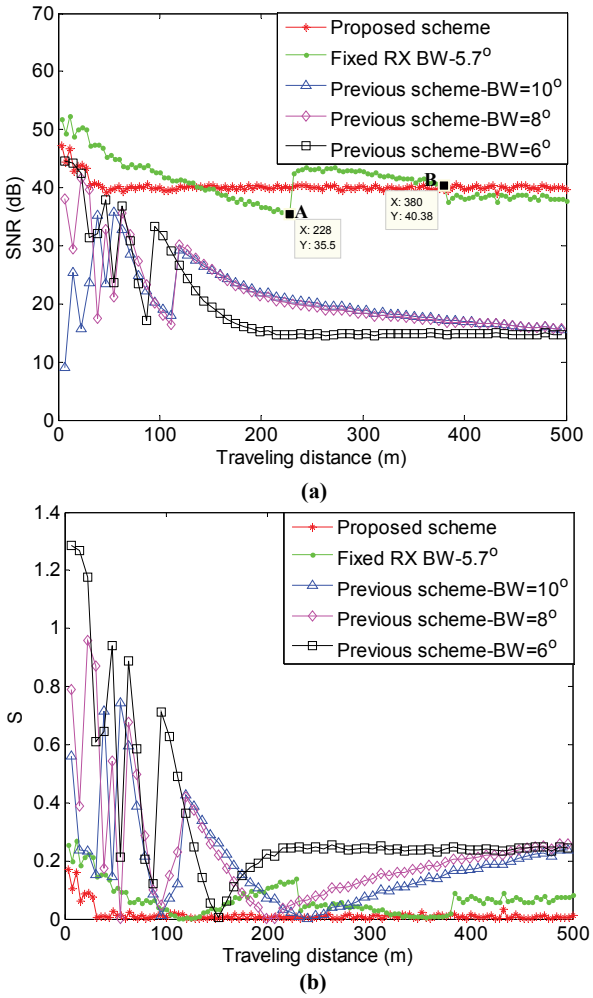

Fig. 9. (a) SNR comparisons, (b) SNR stability comparisons.

V. Conclusions

Following the development paces of public mobile communications, future HSR wireless networks will also be likely to exploit higher frequency bands, even mmWave frequency bands, to enhance the system capacity so as to satisfy the increasing data rate requirements resulting from the rapid progress in the HSR industry. To mitigate the inherent blindness problem in mmWave beamforming networks, we apply the C/U-plane decoupled network architecture to use more reliable lower frequency bands with omnidirectional antennas to assist operations in mmWave bands. Nevertheless, the high mobility in HSR scenarios will still cause frequent beam realignments and consequently high feedback overheads, which significantly influences the transmission reliability and efficiency. In mmWave beamforming networks, besides TXs, RXs are also equipped with antenna arrays, i.e., RXs are also authorized the ability of link adaptation. Based on

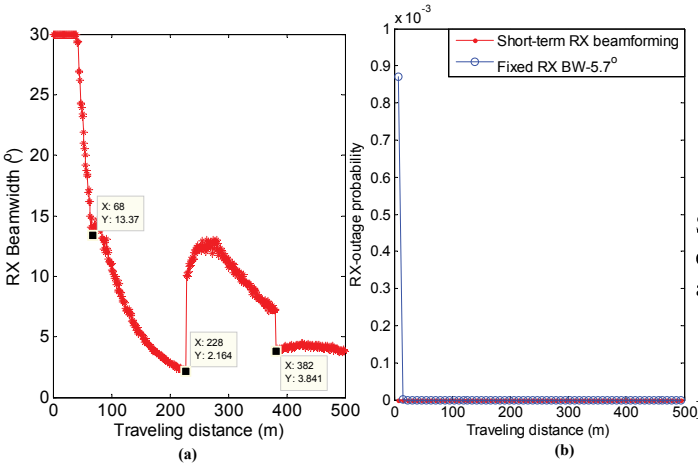

Fig. 10. (a) RX BW of short-term RX beamforming, (b) Communication outage probability resulting from RX beam misalignments .

this observation, we have proposed a stable beamforming scheme with low overhead, consisting of the long-term TX beamforming and the short-term RX beamforming, to solve the above problem. During the long-term TX beamforming, TXs use as wide beam as possible to extend each beam's serving time while satisfying the basic receiver sensitivity. In the short-term RX beamforming, within a TX beam, RXs autonomously adjust RX beams to adapt to diverse wireless channels instead of frequently feeding back CSIs to TXs, reducing feedback overheads and accelerating link adaptations. Finally, the received SNR is kept at a stable and high level, guaranteeing the capacity stability. Theoretical and numerical results have demonstrated the effectiveness of our scheme in reducing feedback overhead while maintaining the capacity stability. It should be noted that for simplicity we describe this scheme based on the downlink. Nevertheless, it also can be generalized to the uplink. In our future work, we will have a deep study on applying this scheme to NLOS scenarios. Besides, how to execute handovers between mmW-RRUs is also a valuable research direction.

Appendix A

To enhance the readability of this paper, some long derivations are moved to the appendices to avoid the fragmentation of the content mainline.

Proof of Proposition 1

In order to reduce feedback overheads, each TX beam radiated from the mmW-RRU is supposed to extend its effective beam coverage as large as possible so as to lower the number of beam switching. Based on this observation, the left and right boundaries of beam 0 should intersect with the track at BSP_0 and BSP_1, respectively. Consequently, the effective beam coverage of TX beam 0 can be calculated as $\tan\left(\theta_{b,0}^{TX}\right)\cdot d_{\min}$. Similarly, the left and right boundaries of beam 1 should intersect with the track at BSP_1 and BSP_2, and we can get the sum of L_0 and L_1 as $\tan\left(\theta_{b,0}^{TX}+\theta_{b,1}^{TX}\right)\cdot d_{\min}$. Consequently, $L_1=\tan\left(\theta_{b,0}^{TX}+\theta_{b,1}^{TX}\right)\cdot d_{\min}-\tan\left(\theta_{b,0}^{TX}\right)\cdot d_{\min}$ is obtained. The rest can be done in the same fashion.

Appendix B

Proof of Proposition 2

Based on the geometric relationships in Fig. 4, we can get

$$\Delta x=\frac{\sin\left(\Delta\mu_i\right)\cdot D_i}{\sin\left(\mu+\Delta\mu_i\right)}. \tag{17}$$

Since Δx is small, its counterpart $\Delta\mu$ is also very small compared with μ. To get a tractable expression between Δx and $\Delta\mu_i$, two approximations are used as follows

$$\begin{aligned}\sin\left(\Delta\mu_i\right)&\approx\Delta\mu_i\\ \sin\left(\mu+\Delta\mu_i\right)&\approx\sin\left(\mu\right)\end{aligned} \tag{18}$$

Based on Fig. 4, it is easy to find that

$$\sin\left(\mu\right)=\frac{d_{\min}}{D_i}. \tag{19}$$

Consequently, at BSP_i we can obtain

$$\Delta x\approx\frac{\Delta\mu_i\cdot D_i^2}{d_{\min}}. \tag{20}$$

Appendix C

Proof of Proposition 6

As shown in (1), the antenna gain pattern has an approximate form of the Gaussian distribution. Therefore,

$$\begin{aligned}&\tfrac{1}{\varpi_i}\int_0^{\varpi_i}G\left(\theta_b^{RX,i},\Delta\theta\right)d\Delta\theta\\ &=\tfrac{1}{\varpi_i}\int_0^{\varpi_i}\tfrac{2\pi}{\theta_b^{RX,i}}e^{-\eta\left(\frac{\Delta\theta}{\theta_b^{RX,i}}\right)^2}d\Delta\theta\\ &=\tfrac{2\pi}{\varpi_i}\sqrt{\tfrac{\pi}{\eta}}\int_0^{\varpi_i}\tfrac{1}{\sqrt{2\pi}\left(\theta_b^{RX,i}/\sqrt{2\eta}\right)}e^{-\frac{\Delta^2\theta}{2\left(\theta_b^{RX,i}/\sqrt{2\eta}\right)^2}}d\Delta\theta\\ &=\tfrac{2\pi}{\varpi_i}\sqrt{\tfrac{\pi}{\eta}}\left(\int_{-\infty}^{\varpi_i}\tfrac{1}{\sqrt{2\pi}\left(\theta_b^{RX,i}/\sqrt{2\eta}\right)}e^{-\frac{\Delta^2\theta}{2\left(\theta_b^{RX,i}/\sqrt{2\eta}\right)^2}}d\Delta\theta-\tfrac{1}{2}\right)\\ &=\tfrac{c}{\varpi_i}\left(\Phi\left(\tfrac{\varpi_i}{\theta_b^{RX,i}/\sqrt{2\eta}}\right)-\tfrac{1}{2}\right)\end{aligned} \tag{21}$$

References

[1] T. Rappaport, S. Sun, R. Mayzus, H. Zhao, Y. Azar, K. Wang, G. Wong, J. Schulz, M. Samimi, and F. Gutierrez, "Millimeter wave mobile communications for 5G cellular: It will work!" *IEEE Access*, vol. 1, pp. 335–349, May 2013.

[2] K. Guan, G. Li, T. Krner, A. F. Molisch, B. Peng, R. He, B. Hui, J. Kim, and Z. Zhong, "On millimeter wave and THz mobile radio channel for smart rail mobility," *IEEE Transactions on Vehicular Technology*, vol. 66, no. 7, pp. 5658–5674, Jul. 2017.

[3] H. Song, X. Fang, and Y. Fang, "Millimeter-wave network architectures for future high-speed railway communications: Challenges and solutions," *IEEE Wireless Communications*, vol. 23, no. 6, pp. 114–122, Dec. 2016.

[4] H. Shokri-Ghadikolaei, C. Fischione, G. Fodor, P. Popovski, and M. Zorzi, "Millimeter wave cellular networks: A MAC layer perspective," *IEEE Transactions on Communications*, vol. 63, no. 10, pp. 3437–3458, Oct. 2015.

[5] L. Yan, X. Fang, and Y. Fang, "Control and data signaling decoupled architecture for railway wireless networks," *IEEE Wireless Communications*, vol. 22, no. 1, pp. 103–111, Feb. 2015.

[6] L. C. Godara, "Applications of antenna arrays to mobile communications. I. Performance improvement, feasibility, and system considerations," *Proceedings of the IEEE*, vol. 85, no. 7, pp. 1031–1060, Jul. 1997.

[7] H. H. Wang and H. A. Hou, "Field trial and study of route-tracking beamforming over high-speed railway," in *Proceeding of* IEEE International Conference on Intelligent Transportation Systems (ITSC), Washington, DC, USA, Oct. 2011, pp. 2063–2067.

[8] M. Cheng, X. Fang, and W. Luo, "Beamforming and positioning-assisted handover scheme for long-term evolution system in high-speed railway," *IET Communications*, vol. 6, no. 15, pp. 2335–2340, Oct. 2012.
[9] W. Luo, X. Fang, M. Cheng, and Y. Zhao, "Efficient multiple-group multiple-antenna (mgma) scheme for high-speed railway viaducts," *IEEE Transactions on Vehicular Technology*, vol. 62, no. 6, pp. 2558–2569, Jul. 2013.
[10] M. R. Akdeniz, Y. Liu, M. K. Samimi, S. Sun, S. Rangan, T. S. Rappaport, and E. Erkip, "Millimeter wave channel modeling and cellular capacity evaluation," *IEEE Journal on Selected Areas in Communications*, vol. 32, no. 6, pp. 1164–1179, Jun. 2014.
[11] Y. Zhao, C. Yin, and J. Li, "Learning-and optimization-based channel estimation for cognitive high-speed rail broadband wireless communications," in *Proceedings of* International Symposium on Communications and Information Technologies (ISCIT), Gold Coast, QLD, Oct. 2012, pp. 562–567.
[12] Y. Cui, X. Fang, and L. Yan, "Hybrid spatial modulation beamforming for mmWave railway communication systems," *IEEE Transactions on Vehicular Technology*, vol. 65, no. 12, pp. 9597–9606, Dec. 2016.
[13] L. Yan, X. Fang, H. Li, and C. Li, "An mmWave wireless communication and radar detection integrated network for railways," in *Proceedings of* 2016 IEEE 83rd Vehicular Technology Conference (VTC Spring), Nanjing, China, May 2016, pp. 1–5.
[14] D. Chizhik, "Slowing the time-fluctuating MIMO channel by beamforming," *IEEE Transactions on Wireless Communications*, vol. 3, no. 5, pp. 1554–1565, Sept 2004.
[15] S. Soltani, K. Misra, and H. Radha, "On link-layer reliability and stability for wireless communication," in *Proceedings of* 14th ACM international conference on Mobile computing and networking, San Francisco, California, USA, Sept. 2008, pp. 327–338.
[16] Y. Tian, K. Xu, and N. Ansari, "TCP in wireless environments: problems and solutions," *IEEE Communications Magazine*, vol. 43, no. 3, pp. S27–S32, Mar. 2005.
[17] G. P. White and Y. V. Zakharov, "Data communications to trains from high-altitude platforms," *IEEE Transactions on Vehicular Technology*, vol. 56, no. 4, pp. 2253–2266, Jul. 2007.
[18] V. Vakilian, J. F. Frigon, and S. Roy, "Effects of angle-of-arrival estimation errors, angular spread and antenna beamwidth on the performance of reconfigurable SISO systems," in *Proceedings of* IEEE Pacific Rim Conference on Communications, Computers and Signal Processing, Victoria, BC, Canada, Aug. 2011, pp. 515–519.
[19] Wikipedia.(2017 Apr.).[online].Available:https://en.wikipedia.org/wiki/Q-function.
[20] M. Marcus and B. Pattan, "Millimeter wave propagation: spectrum management implications," *IEEE Microwave Magazine*, vol. 6, no. 2, pp. 54–62, Jun. 2005.
[21] Y. H. Nam, Y. Akimoto, Y. Kim, M. i. Lee, K. Bhattad, and A. Ekpenyong, "Evolution of reference signals for LTE-advanced systems," *IEEE Communications Magazine*, vol. 50, no. 2, pp. 132–138, February 2012.
[22] J. Kim and I. G. Kim, "Distributed antenna system-based millimeter-wave mobile broadband communication system for high speed trains," in *Proceedings of* 2013 International Conference on ICT Convergence (ICTC), Jeju, South Korea, Oct. 2013, pp. 218–222.
[23] E. Dahlman, S. Parkvall, and J. Sköld, LTE/LTE-Advanced for Mobile Broadband. Elsevier Ltd, 2011.
[24] J. Kim, H. S. Chung, I. G. Kim, H. Lee, and M. S. Lee, "A study on millimeter-wave beamforming for high-speed train communication," in *Proceedings of* 2015 International Conference on Information and Communication Technology Convergence (ICTC), Jeju, South Korea, Oct. 2015, pp. 1190–1193.

Li Yan (S'14) received the B.E. degree in communication engineering from Southwest Jiaotong University, Chengdu, China, where she is currently pursuing the Ph.D. degree with the Key Laboratory of Information Coding and Transmission, School of Information Science and Technology. She is now a visiting student in the Department of Electrical and Computer Engineering, University of Florida, USA. Her research interests include 5G communications, mobility managements, network architecture, and HSR wireless communications.

Xuming Fang (SM'16) received the B.E. degree in electrical engineering in 1984, the M.E. degree in computer engineering in 1989, and the Ph.D. degree in communication engineering in 1999 from Southwest Jiaotong University, Chengdu, China. He was a Faculty Member with the Department of Electrical Engineering, Tongji University, Shanghai, China, in September 1984. He then joined the School of Information Science and Technology, Southwest Jiaotong University, Chengdu, where he has been a Professor since 2001, and the Chair of the Department of Communication Engineering since 2006. He held visiting positions with the Institute of Railway Technology, Technical University at Berlin, Berlin, Germany, in 1998 and 1999, and with the Center for Advanced Telecommunication Systems and Services, University of Texas at Dallas, Richardson, in 2000 and 2001. He has, to his credit, around 200 high-quality research papers in journals and conference publications. He has authored or coauthored five books or textbooks. His research interests include wireless broadband access control, radio resource management, multihop relay networks, and broadband wireless access for high speed railway. Dr. Fang is the Chair of IEEE Vehicular Technology Society of Chengdu Chapter.

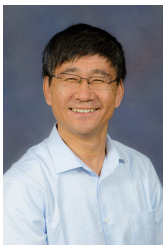

Yuguang "Michael" Fang (F'08) received a BS/MS degree from Qufu Normal University, Shandong, China in 1987, a Ph.D degree from Case Western Reserve University in 1994 and a Ph.D. degree from Boston University in 1997. He joined the Department of Electrical and Computer Engineering at University of Florida in 2000 and has been a full professor since 2005. He holds a University of Florida Research Foundation (UFRF) Professorship from 2006 to 2009, a Changjiang Scholar Chair Professorship with Xidian University, China, from 2008 to 2011, and a Guest Chair Professorship with Tsinghua University, China, from 2009 to 2012.

Dr. Fang received the US National Science Foundation Career Award in 2001 and the Office of Naval Research Young Investigator Award in 2002, and is the recipient of the Best Paper Award from IEEE ICNP (2006). He has also received a 2010-2011 UF Doctoral Dissertation Advisor/Mentoring Award, 2011 Florida Blue Key/UF Homecoming Distinguished Faculty Award, and the 2009 UF College of Engineering Faculty Mentoring Award. He was the Editor-in-Chief of IEEE Transactions on Vehicular Technology (2013-2017), the Editor-in-Chief of IEEE Wireless Communications (2009-2012) and serves/served on several editorial boards of journals including IEEE Transactions on Mobile Computing (2003-2008, 2011-present), IEEE Transactions on Communications (2000-2011), and IEEE Transactions on Wireless Communications (2002-2009). He has been actively participating in conference organizations such as serving as the Technical Program Co-Chair for IEEE INOFOCOM2014 and the Technical Program Vice-Chair for IEEE INFOCOM'2005. He is a fellow of the IEEE.